

Communication

Single-Step Synthesis Process for High-Entropy Transition Metal Boride Powders Using Microwave Plasma

Bria Storr ¹, Deepa Kodali ², Kallol Chakrabarty ¹, Paul A. Baker ¹, Vijaya Rangari ²
and Shane A. Catledge ^{1,*}¹ Department of Physics, University of Alabama at Birmingham, Birmingham, AL 35294-1170, USA; bcstorr@uab.edu (B.S.); kallol89@uab.edu (K.C.); pabaker@uab.edu (P.A.B.)² Department of Materials Science & Engineering, Tuskegee University, Tuskegee, AL 36088-1923, USA; dkodali@tuskegee.edu (D.K.); vrangari@tuskegee.edu (V.R.)

* Correspondence: catledge@uab.edu

Abstract: A novel approach is demonstrated for the synthesis of the high entropy transition metal boride (Ta, Mo, Hf, Zr, Ti)_{B₂} using a single heating step enabled by microwave-induced plasma. The argon-rich plasma allows rapid boro-carbothermal reduction of a consolidated powder mixture containing the five metal oxides, blended with graphite and boron carbide (B₄C) as reducing agents. For plasma exposure as low as 1800 °C for 1 h, a single-phase hexagonal AlB₂-type structure forms, with an average particle size of 165 nm and with uniform distribution of the five metal cations in the microstructure. In contrast to primarily convection-based (e.g., vacuum furnace) methods that typically require a thermal reduction step followed by conversion to the single high-entropy phase at elevated temperature, the microwave approach enables rapid heating rates and reduced processing time in a single heating step. The high-entropy phase purity improves significantly with the increasing of the ball milling time of the oxide precursors from two to eight hours. However, further improvement in phase purity was not observed as a result of increasing the microwave processing temperature from 1800 to 2000 °C (for fixed ball milling time). The benefits of microwave plasma heating, in terms of allowing the combination of boro-carbothermal reduction and high entropy single-phase formation in a single heating step, are expected to accelerate progress in the field of high entropy ceramic materials.

Keywords: high-entropy; microwave; plasma; ceramics; boride

Citation: Storr, B.; Kodali, D.; Chakrabarty, K.; Baker, P.A.; Rangari, V.; Catledge, S.A. Single-Step Synthesis Process for High-Entropy Transition Metal Boride Powders Using Microwave Plasma. *Ceramics* **2021**, *4*, 257–264. <https://doi.org/10.3390/ceramics4020020>

Academic Editors: Angel L. Ortiz and Gilbert Fantozzi

Received: 9 April 2021

Accepted: 24 May 2021

Published: 28 May 2021

Publisher's Note: MDPI stays neutral with regard to jurisdictional claims in published maps and institutional affiliations.



Copyright: © 2021 by the authors. Licensee MDPI, Basel, Switzerland. This article is an open access article distributed under the terms and conditions of the Creative Commons Attribution (CC BY) license (<https://creativecommons.org/licenses/by/4.0/>).

1. Introduction

The recent spotlight on high entropy alloys is driven by outstanding properties such as enhanced fracture toughness, tensile strength, as well as corrosion and high temperature oxidation resistance [1]. In 2016, the fabrication of single-phase high-entropy borides (HEBs) in the hexagonal AlB₂ structure was first reported [2], representing the first non-oxide high-entropy ceramic fabricated in bulk form. They have a uniquely layered hexagonal crystal structure with alternating rigid 2D boron nets and high-entropy 2D layers of metal cations characterized by mixed ionic and covalent metal–boron bonds. Thermodynamic stability is one of the hallmarks of high entropy materials as the high entropy can provide phase stability, particularly at high temperature, due to minimization of Gibbs free energy. Ultra-high temperature ceramics have applications including cutting tools, molten metal containments, microelectronics and aerospace components [3,4]. Because of the potential for entropy stabilization in ceramics, high entropy ultra-high temperature ceramics (e.g., borides and carbides) are being considered as candidates for materials in extreme conditions, such as is needed in hypersonic or atmospheric re-entry vehicles, rocket propulsion, etc. [5].

Multiple heating steps that rely primarily on convective heating (e.g., via vacuum furnace) are often used to reduce the precursor metal oxide powder via Boro-CarboThermal

Reduction (BCTR), followed by subsequent heating and or heating/sintering steps to finally convert the reduced mixture into the single-phase HEB [5–7]. In this work, HEB synthesis is reported via BCTR of a five-component transition metal oxide powder mixture (with B_4C and graphite reducing agents) efficiently performed as a single step by application of low temperature microwave (MW) plasma.

A low temperature plasma represents a unique state of matter composed of neutral atoms and molecules, radicals, excited states, ions and electrons with characteristic electron energies of a few eV to 10 eV and low degrees of ionization [8]. The energetic electrons can efficiently generate radicals, charged species, excited states and photons. Microwave heating of powdered metals was pioneered in 1999 and has gained popularity in the field of sintering powder metallurgy products [9] and even primary metallurgy [10]. Scientific literature regarding the use of microwaves to prepare high entropy alloys was first reported in 2011 for combustion synthesis of FeCoNiCuAl [11]. However, to the best of our knowledge, no MW or MW-plasma approach has yet been reported for synthesis of HE ceramics including diborides.

In our approach, rapid plasma heating (70–100 °C/min) takes place with energetic particles recombining and depositing large amounts of energy to the ceramic. The dielectric nature of the metal-oxide precursor powder strongly absorbs energy from the electric field component of MWs via dipolar polarization to volumetrically heat the sample. The MW frequencies can penetrate and deposit heat in the interior of the ceramic, thus reversing the usual outside-in temperature gradient seen in conventional radiant heating. While primarily intended as a reducing agent, the presence of graphite in the precursor powder also enables conductive heating as electric currents can form in response to mobile charge carriers to aid in the distribution of heat throughout the ceramic. Both heating mechanisms (dipolar polarization and conduction) are found to be important in systems that include a conducting material scattered in a non-conducting medium (e.g., electrolyte solutions) [12]. Finally, the plasma discharge can exert a significant effect in promoting microwave heating processes and chemical reactions as highly active species such as electrons, ions and radicals can significantly enhance the reaction rate [13]. Overall, the MW plasma approach is advantageous due to enhanced diffusion processes, reduced energy consumption, very rapid heating rates and considerably reduced processing times, decreased sintering temperatures, improved physical and mechanical properties, simplicity, and lower environmental hazards—features that have not been observed in conventional processes [14–17].

2. Materials and Methods

The precursor powders included five metal oxides: hafnium oxide (HfO_2 : 99%, 325-mesh; Alfa Aesar), zirconium oxide (ZrO_2 : 99+%, 325-mesh; Alfa Aesar), tantalum pentoxide (Ta_2O_5 : 99%, 60-mesh; Alfa Aesar), titanium oxide (TiO_2 : 99.6%, 325-mesh; Alfa Aesar), Molybdenum oxide (MoO_3 , 99.95%, 325-mesh; Alfa Aesar), carbon black (C: 99.9+%, mesh size not provided by manufacturer; Alfa Aesar) and boron carbide (B_4C , 99+%, 325-mesh; Alfa Aesar). Appropriate amounts of the precursor powders were chosen, with stoichiometry being calculated from the metal basis in an attempt to produce an equimolar diboride given as: $(Hf_{0.2}, Zr_{0.2}, Ti_{0.2}, Ta_{0.2}, Mo_{0.2})B_2$. As is typically reported for BCTR [6,18], an excess of B_4C was added to compensate for the loss of B due to evaporation of volatile boron oxide species during synthesis. Precursor powders were milled using a high energy ball mill (Spex 8000 M, Metuchen, NJ, USA) with a tungsten carbide (WC)-lined cylindrical sample vial of 2.25 inch diameter and 2.5 inch length. The shaking pattern is a complex motion that combines back-and-forth swings with short lateral movements, each end of the vial describing a “figure-8”. The clamp speed was 1060 cycles per minute. First, the five metal oxides were combined with carbon black and dry milled using two WC balls (7/16 inch diameter) for 2 h. Different total milling times were evaluated in this study (from 0 to 8 h) with the first 2 h always using the dry milling with WC balls. For samples milled for greater than 2 h, the remaining time made use of wet milling with two ZrO_2 balls (1/2 inch diameter) in acetone. The ball to powder weight ratio for dry

milling was approximately 2:1 and, for wet milling, was 1:1. The mixture was dried at room temperature in a vacuum oven, passed through a 200-mesh sieve, and then combined with B₄C and sieved once again. Finally, the mixture was consolidated into a disk with a diameter of 5 mm under a uniaxial pressure of 50 MPa.

For the MW plasma process, the consolidated powder disk was placed on a molybdenum stage in a vacuum chamber (Wavemat Inc., Plymouth, MI, USA; details in [19]) and pumped to a base pressure of 1.3 Pa prior to MW processing. An argon-rich feedgas mixture (50 sccm Ar, 50 sccm H₂) was then added to the chamber and the plasma was ignited by a 2.45 GHz magnetron. The addition of H₂ was found to be necessary to concentrate and stabilize the plasma around the sample while minimizing reflected microwave power. The heating rate of the sample was measured to be 70–100 °C/min. The temperature of the sample disk, adjustable by microwave power (1.3–1.5 kW) and chamber pressure (2.4×10^4 – 3.3×10^4 Pa, controlled via exhaust throttle valve), was monitored by optical pyrometry to evaluate its effect on HEB formation by conducting experiments at 1800 °C or at 2000 °C for one hour.

The specimens were characterized by X-ray diffraction (XRD), transmission electron microscopy (TEM), and by scanning electron microscopy (SEM) in conjunction with energy dispersive X-ray spectroscopy (EDX). An X-ray diffractometer (Malvern Panalytical, model Empyrean, Netherlands) with Cu K α radiation ($\lambda = 1.54186 \text{ \AA}$) was used at 45 kV and 40 mA, with 16.32 s per step and 0.0131° step size. A TEM (JEOL, model 2010, Peabody, MA, USA) unit was used. The consolidated disks were ground using a mortar and pestle, sieved using 200-mesh and dispersed in ethanol, and then 1 μ L of the suspension was deposited onto a copper grid and observed in TEM at an operating voltage of 200 kV. An SEM (FEI Quanta FEG 650, Hillsboro, OR, USA) was used for collecting SEM/EDX images at an accelerating voltage of 15 kV.

3. Results and Discussion

Pressure consolidated disk samples of the precursor powder mixture were exposed to the MW plasma to achieve disk temperatures of 2000 °C and 1800 °C for 1 h; the resulting XRD patterns are shown in Figure 1a,b, respectively. The XRD of the starting precursor powder mixture containing the metal oxides, graphite and boron carbide after ball milling is shown in Figure 1c. The samples processed at 2000 °C and 1800 °C both reveal the hexagonal AlB₂-type phase structure that is characteristic of the high-entropy diboride. However, the sample processed at 1800 °C shows incomplete transformation with remaining intermediate phases. These include several solid solutions of binary metal borides such as (Hf,Zr)B₂ resulting in a broadening of the primary HEB peaks, with a tail on the low-2 θ side, as well as cubic TaC. Reports on the BCTR synthesis of HEBs have also shown secondary phase formation, including binary borides, at lower annealing temperature [6,18]. In contrast, the sample processed at 2000 °C has much sharper HEB peaks, with only very minor secondary phases, indexed primarily to excess B₄C that was used in the precursor mixture. The XRD patterns were analyzed using Rietveld refinement to calculate the lattice parameters and unit cell volume based on the hexagonal AlB₂-type phase structure with space group P6/mmm. The results are summarized in Table 1. The unit cell volume for the HEB sample produced at 2000 °C in the present study is about 1.5% lower than that predicted in a previous computational study for the same HEB material composition [20]. The unit cell volume from other reported experimental results for this HEB material composition, made using either BCTR followed by sintering [6] or by using mechanical alloying of borides followed by sintering [2], are also provided in Table 1. Considering the five binary metal diborides individually, the unit cell volume for TaB₂ (26.760 \AA^3 ; PDF # 01-076-0966) comes closest to our experimentally determined value (27.767 \AA^3), with a difference of 3.5%.

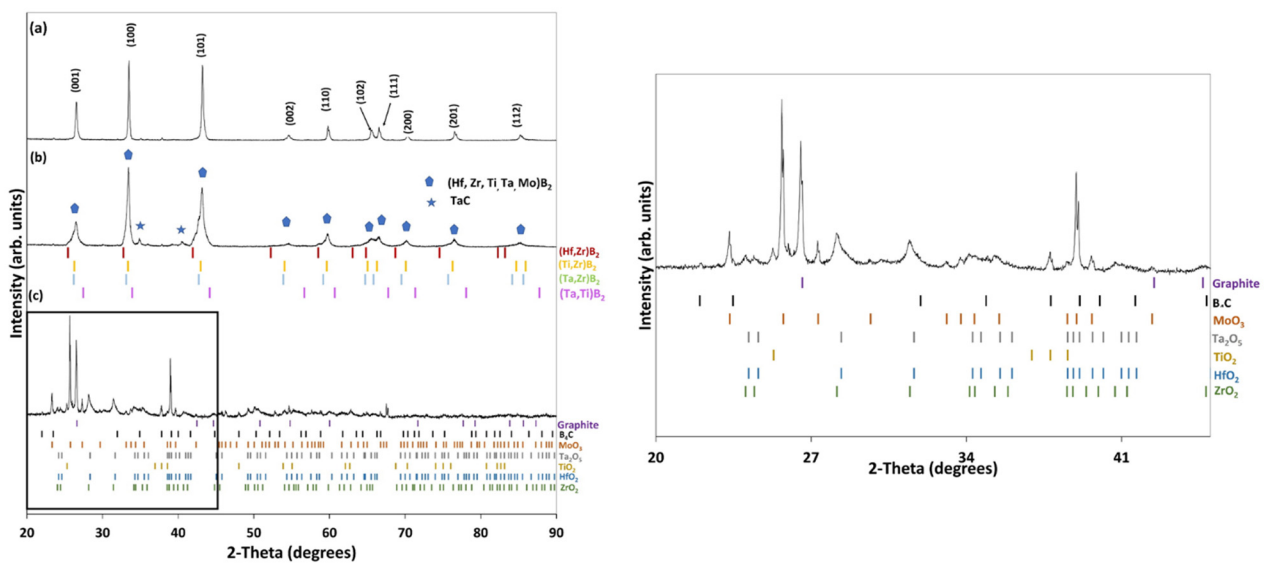


Figure 1. XRD of MW-plasma samples processed at (a) 2000 °C and (b) 1800 °C, and (c) the starting precursor mixture of 5-metal oxides + graphite + B₄C. Vertical bars represent Crystallographic Open database (COD) entries for: ZrO₂ (96-901-6715); Ta₂O₅ (96-901-4282); HfO₂ (96-901-3471); TiO₂ (96-900-9087); MoO₃ (96-900-9670); B₄C (96-412-4698); Graphite (96-901-2233); (Hf,Zr)B₂(96-151-0842); (Hf,Ti)B₂ (96-151-0711); (Ta,Zr)B₂ (96-151-0838); (Ti,Zr)B₂ (96-151-0846); (Ta,Ti)B₂ (96-151-0836). A zoomed-in region of (c) is provided for clarity.

Table 1. Measured lattice parameters of the HEB samples at 1800 °C and 2000 °C, along with those found from three other references.

	HEB-1800 °C	HEB-2000 °C	Ref [20]	Ref [6]	Ref [2]
c-axis (Å)	3.368	3.358	3.376	3.366	3.316
a-axis (Å)	3.085	3.090	3.105	3.092	3.080
Unit cell volume (Å ³)	27.760	27.767	28.187	27.869	27.242
c/a ratio	1.091	1.086	1.087	1.089	1.077

To further support the claim of the solid solution nature of the synthesized HEB, SEM/EDX compositional maps were obtained for each of the metal components in the structure. The consolidated disk for the sample made at 2000 °C was lightly ground using a mortar/pestle for subsequent imaging of individual coarse particles. SEM images and the corresponding EDX compositional maps for each metallic component for this sample are shown in Figure 2. The secondary electron image in Figure 2a shows a broad distribution of particle size (100 nm–10 μm) as some degree of particle sintering occurs during the MW plasma process. The EDX maps reveal a homogeneous distribution of each of the five metallic components, consistent with a single-phase solid solution HEB structure, as revealed by the XRD data in Figure 1a. This, combined with no strong secondary metal oxides, binary metal borides, or intermetallic phases in the XRD pattern, supports our conclusion that a nearly single-phase solid solution HEB phase is formed.

Ball milling is known to strongly influence subsequent reactions during alloying and sintering processes [21], but its effect on MW plasma processing of HEB ceramics is not well known. To further investigate the role of ball milling on subsequent MW plasma processing, a range of ball milling times was explored from 0 h to 8 h, and then the consolidated disks were exposed to MW plasma for 1 h at 1800 °C. As shown in Figure 3, with 0 h ball milling of the precursor powder, the HEB structure could not form. This was also the case for 2000 °C MW plasma processing temperature. However, an improvement in HEB phase purity (indicated by reduced presence of secondary phases) occurs for longer ball milling time. For 8 h ball milling, the single-phase HEB forms with very minimal secondary

phases present. These data (along with those in Figure 1) suggest that longer ball milling times could possibly allow the single phase HEB to be achieved at MW plasma processing temperatures below 1800 °C.

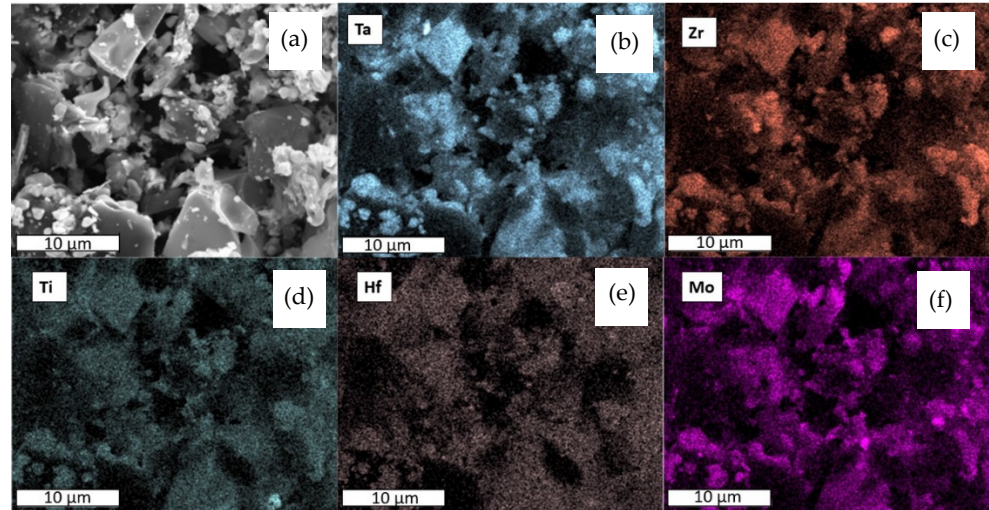


Figure 2. Scanning electron microscopy (SEM) micrograph (a) with corresponding EDX elemental maps for (b) Ta, (c) Zr, (d) Ti, (e) Hf, and (f) Mo of the HEB sample produced at 2000 °C after loosely grinding into a powder with no sieving.

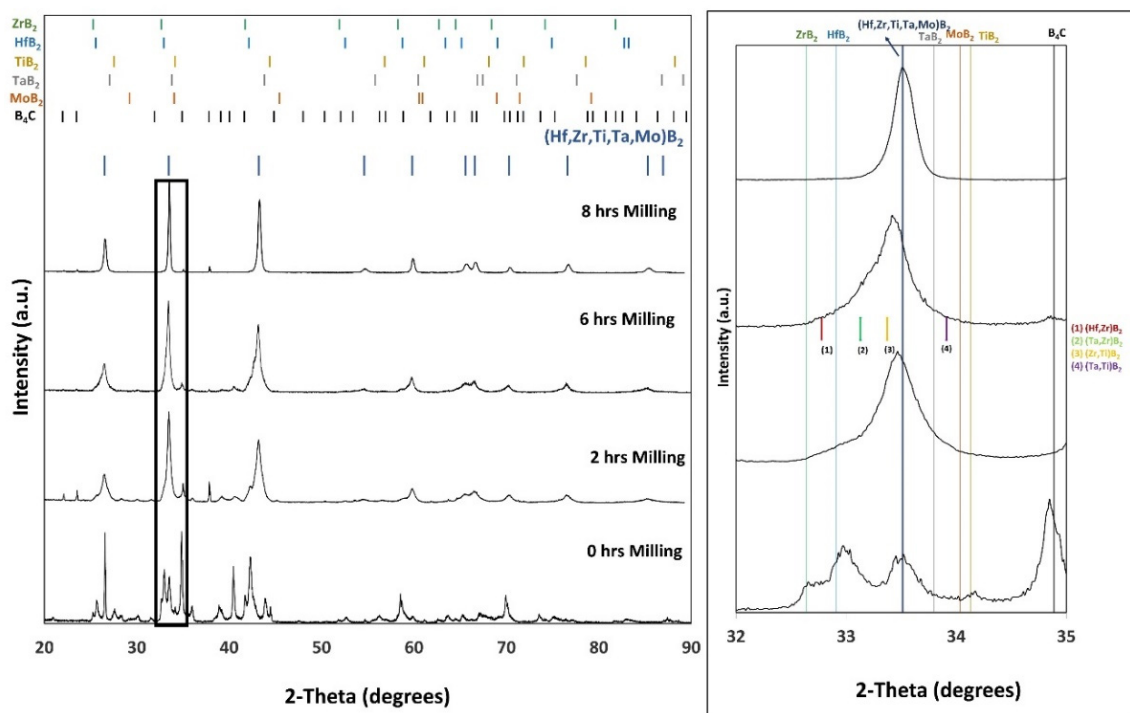


Figure 3. XRD of samples ball milled for different times (0 to 8 h) and exposed to MW plasma to achieve a disk temperature of 1800 °C. The first two hours of ball milling were dry and the remaining time was completed via wet milling, as specified in Section 2. Vertical bars represent Crystallographic Open database (COD) entries for: ZrB_2 (96-151-0857); TaB_2 (96-151-0839); HfB_2 (96-151-0712); TiB_2 (96-100-9059); MoB_2 (96-200-2800); B_4C (96-412-4698). A zoomed-in region for 2-theta between 32 and 35 degrees is provided for clarity.

In order to further characterize particle/grain size of the MW plasma processed samples, both SEM and TEM were performed after grinding the consolidated disks and ultrasonically dispersing the powder in ethanol. Figure 4 shows (a) TEM and (b) SEM of the HEB sample ball milled for 8 h and then MW processed at 1800 °C for 1 h. From TEM, some individual grains can be discerned, with an estimated average size of 20 nm. The SEM micrograph with histogram shows an average particle size of 165 nm. A Gaussian distribution was used to obtain the mean particle size. The significant difference in SEM/TEM particle size is due to agglomeration during preparation of samples for SEM. One of the potential benefits of MW processing of ceramic materials is a reduction in sintering temperature, which can translate into reduced grain growth and an improvement in the final sintered density [14]. Future work will include efforts to reduce the MW plasma processing temperature to below 1800 °C, and to evaluate the subsequent sinterability and final compact density of resulting HEB structures.

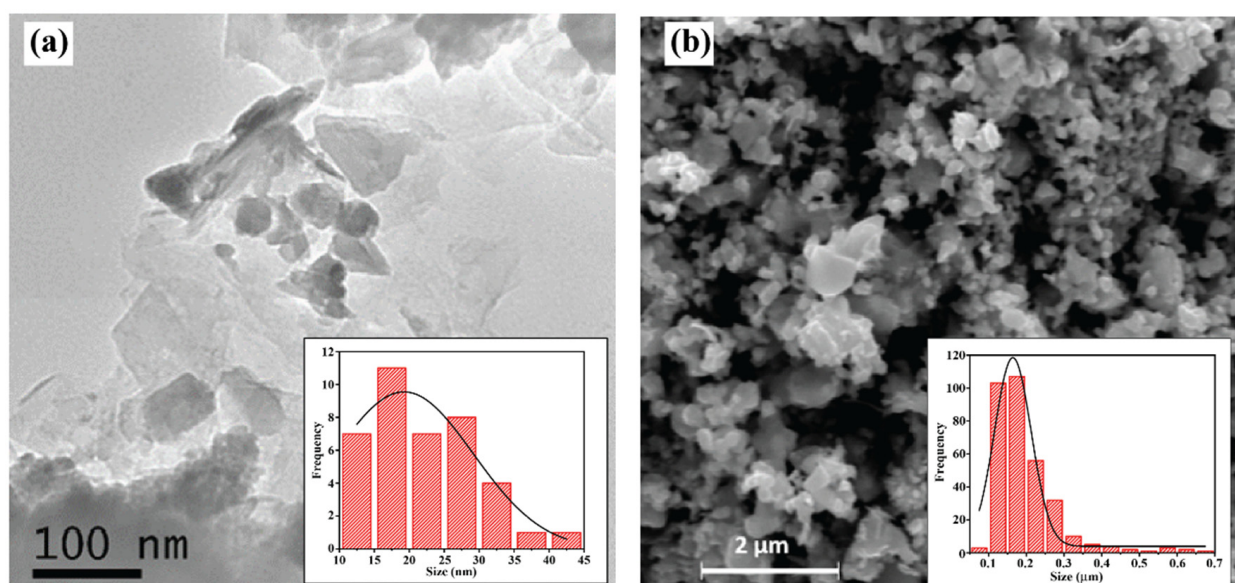


Figure 4. Micrographs of MW plasma processed HEB samples obtained from (a) TEM and (b) SEM with the particle size distribution in the inset.

4. Conclusions

This work demonstrates a novel approach, involving a single heating step, for the efficient synthesis of a high entropy diboride (Hf, Zr, Ti, Ta, Mo) B_2 using low-temperature microwave plasma to initiate and complete the boro-carbothermal reduction of metal-oxide precursors. This differs from prior reports of HEB synthesis that typically use multiple steps of convection-based heating, followed by sintering at elevated pressures/temperatures, to complete the HEB phase transformation. The MW plasma process results in the HEB phase with minimal secondary phase formation, for sample temperatures as low as 1800 °C, for 1 h. This, combined with no substantial secondary metal oxides, binary metal borides, or intermetallic phases in the XRD pattern, supports our conclusion that a nearly single-phase solid solution HEB phase is formed. XRD diffraction with Rietveld analysis yields unit cell volumes that are commensurate with the same HEB composition found in prior computational work and in experimental studies that use conventional heating/sintering approaches. Reduction to the HEB phase was found to be aided by longer ball milling time, allowing a lower MW plasma processing temperature to be used. When no ball milling of the precursor mixture was performed, the HEB phase did not form, regardless of the MW process temperatures investigated in this study. The role of the plasma in this process is not yet fully understood and warrants further investigation as a means to potentially accelerate the kinetics for HEB formation at even lower sample temperatures and/or MW processing times.

Author Contributions: Conceptualization, S.A.C.; methodology, S.A.C. and B.S.; validation, K.C. and B.S.; formal analysis, B.S., S.A.C., D.K., and P.A.B.; investigation, B.S., K.C., and S.A.C.; data curation, B.S.; writing—original draft preparation, B.S.; writing—review and editing, S.A.C.; supervision, S.A.C. and V.R.; funding acquisition, S.A.C. All authors have read and agreed to the published version of the manuscript.

Funding: This research was funded by the National Science Foundation (NSF) EPSCoR RII-Track-1 Cooperative Agreement No. OIA-1655280. Any opinions, findings, and conclusions or recommendations expressed in this material are those of the authors and do not necessarily reflect the views of the National Science Foundation. The authors thank Paul A. Baker for assistance with SEM/EDS measurements.

Institutional Review Board Statement: Not Applicable.

Informed Consent Statement: Not Applicable.

Data Availability Statement: The data presented in this study are available on request from the corresponding author.

Conflicts of Interest: The authors declare no conflict of interest. The funders had no role in the design of the study; in the collection, analyses, or interpretation of data; in the writing of the manuscript, or in the decision to publish the results.

References

1. Tsai, M.-H.; Yeh, J.-W. High-Entropy Alloys: A Critical Review. *Mater. Res. Lett.* **2014**, *2*, 107–123. [[CrossRef](#)]
2. Gild, J.; Zhang, Y.; Harrington, T.; Jiang, S.; Hu, T.; Quinn, M.C.; Mellor, W.M.; Zhou, N.; Vecchio, K.; Luo, J. High-Entropy Metal Diborides: A New Class of High-Entropy Materials and a New Type of Ultrahigh Temperature Ceramics. *Sci. Rep.* **2016**, *6*, 37946. [[CrossRef](#)] [[PubMed](#)]
3. Barbarossa, S.; Orrù, R.; Garroni, S.; Licheri, R.; Cao, G. Ultra high temperature high-entropy borides: Effect of graphite addition on oxides removal and densification behaviour. *Ceram. Int.* **2021**, *47*, 6220–6231. [[CrossRef](#)]
4. Mayrhofer, P.H.; Kirnbauer, A.; Ertelthaler, P.; Koller, C.M. High-entropy ceramic thin films; A case study on transition metal diborides. *Scr. Mater.* **2018**, *149*, 93–97. [[CrossRef](#)]
5. Feng, L.; Fahrenholtz, W.G.; Brenner, D.W. High-Entropy Ultra-High-Temperature Borides and Carbides: A New Class of Materials for Extreme Environments. *Annu. Rev. Mater. Res.* **2021**, *51*. [[CrossRef](#)]
6. Gild, J.; Wright, A.; Quiambao-Tomko, K.; Qin, M.; Tomko, J.A.; Hoque, M.S.b.; Braun, J.L.; Bloomfield, B.; Martinez, D.; Harrington, T.; et al. Thermal conductivity and hardness of three single-phase high-entropy metal diborides fabricated by borocarbothermal reduction and spark plasma sintering. *Ceram. Int.* **2020**, *46*, 6906–6913. [[CrossRef](#)]
7. Gu, J.; Zou, J.; Sun, S.-K.; Wang, H.; Yu, S.-Y.; Zhang, J.; Wang, W.; Fu, Z. Dense and pure high-entropy metal diboride ceramics sintered from self-synthesized powders via boro/carbothermal reduction approach. *Sci. China Mater.* **2019**, *62*, 1898–1909. [[CrossRef](#)]
8. Adamovich, I.; Baalrud, S.D.; Bogaerts, A.; Bruggeman, P.J.; Cappelli, M.; Colombo, V.; Czarnetzki, U.; Ebert, U.; Eden, J.G.; Favia, P.; et al. Vardelle The 2017 Plasma Roadmap: Low temperature plasma science and technology. *J. Phys. D Appl. Phys.* **2017**, *50*, 323001. [[CrossRef](#)]
9. Gupta, M.; Wong, E. *Microwaves and Metals*, 1st ed.; Wiley: Singapore, 2007.
10. Yang, J.; Huang, M.; Peng, J. Microwave Heating for Metallurgical Engineering. In *Electromagnetic fields: Principles, Engineering Applications and Biophysical Effects*; Kwang, M.H., Yoon, S.O., Eds.; Nova Science Publishers Inc.: New York, NY, USA, 2013; ISBN 978-1-62417-063-8.
11. Veronesi, P.; Rosa, R.; Colombini, E.; Leonelli, C. Microwave-Assisted Preparation of High Entropy Alloys. *Technologies* **2015**, *3*, 182–197. [[CrossRef](#)]
12. Horikoshi, S.; Sumi, T.; Serpone, N. Unusual Effect of the Magnetic Field Component of the Microwave Radiation on Aqueous Electrolyte Solutions. *J. Microw. Power Electromagn. Energy* **2012**, *46*, 215–228. [[CrossRef](#)] [[PubMed](#)]
13. Sun, J.; Wang, W.; Yue, Q. Review on Microwave-Matter Interaction Fundamentals and Efficient Microwave-Associated Heating Strategies. *Materials* **2016**, *9*, 231. [[CrossRef](#)] [[PubMed](#)]
14. Yadoji, P.; Peledmedu, R.; Agrawal, D.; Roy, R. Microwave sintering of Ni–Zn ferrites: Comparison with conventional sintering. *Mater. Sci. Eng. B* **2003**, *98*, 269–278. [[CrossRef](#)]
15. Leonelli, C.; Veronesi, P.; Denti, L.; Gatto, A.; Iuliano, L. Microwave assisted sintering of green metal parts. *J. Mater. Process. Technol.* **2008**, *205*, 489–496. [[CrossRef](#)]
16. Menezes, R.; Souto, P.M.; Kiminami, R.H.G.A. Microwave hybrid fast sintering of porcelain bodies. *J. Mater. Process. Technol.* **2007**, *190*, 223–229. [[CrossRef](#)]
17. Clark, D.E.; Folz, D.C.; West, J.K. Processing materials with microwave energy. *Mater. Sci. Eng. A* **2000**, *287*, 153–158. [[CrossRef](#)]

18. Feng, L.; Fahrenholtz, W.G.; Hilmas, G.E. Two-step synthesis process for high-entropy diboride powders. *J. Am. Ceram. Soc.* **2020**, *103*, 724–730. [[CrossRef](#)]
19. Chakrabarty, K.; Arnold, I.; Catledge, S.A. Hexagonal boron nitride grown using high atomic boron emission during microwave plasma chemical vapor deposition. *J. Vac. Sci. Technol. A* **2019**, *37*, 061507. [[CrossRef](#)]
20. Wang, Y.-P.; Gan, G.-Y.; Wang, W.; Yang, Y.; Tang, B.-Y. Ab Initio Prediction of Mechanical and Electronic Properties of Ultrahigh Temperature High-Entropy Ceramics (Hf_{0.2}Zr_{0.2}Ta_{0.2}M_{0.2}Ti_{0.2})B₂ (M = Nb, Mo, Cr). *Phys. Status Solidi (B)* **2018**, *255*, 1800011. [[CrossRef](#)]
21. Suryanarayana, C. Mechanical alloying: A novel technique to synthesize advanced materials. *Research* **2019**, 4219812. [[CrossRef](#)] [[PubMed](#)]